

Sodium Channel Gating Currents

Origin of the Rising Phase

JOSEPH R. STIMERS, FRANCISCO BEZANILLA, and
ROBERT E. TAYLOR

From the Marine Biological Laboratory, Woods Hole, Massachusetts 02543

ABSTRACT There has been some uncertainty in the past as to the origin of the rising phase of the gating current. We present evidence here that proves that the gating current does not have a rising phase and that the observed rising phase is due to an uncompensated series resistance in the Frankenhaeuser-Hodgkin (F-H) space. When a squid giant axon is bathed in a solution that is 10–20% hyperosmotic with respect to the internal solution, the rising phase of the gating current is eliminated. In parallel with this, a component of the capacity transient (time constant, 20 μ s) is reduced so that the capacity transient now appears to be closer to a single fast (5–10 μ s) component. These changes in the capacity transient and gating current occur without altering the amount of charge moved in either. This indicates that the charge is simply redistributed in time. The gating current without a rising phase can still be immobilized by inactivation. Supporting evidence is provided by measuring the accumulation and washout of K^+ from the F-H space. It was found that K^+ washes out 35% faster when the axon is bathed in hyperosmotic solution. It was estimated that the F-H space thickness (θ) increased 2.5 ± 0.4 -fold (mean \pm SEM) in hyperosmotic solution. Similarly, K^+ accumulation in the F-H space was decreased, leading to an estimate of a 5 ± 1.4 -fold increase in θ in hyperosmotic solution. These results are consistent with the simple structural model presented.

INTRODUCTION

Molecular rearrangement of intramembranous charged particles associated with the voltage-dependent opening of Na channels in the squid giant axon produces a measurable gating current (I_g) (Armstrong and Bezanilla, 1973, 1974; Keynes and Rojas, 1973, 1974; Meves, 1974). Since I_g reflects the transition of the channel between conformations that include all the closed states and the open state(s), it provides information that cannot be obtained as readily from macro-

Address reprint requests to Dr. F. Bezanilla, Dept. of Physiology, Ahmanson Laboratory of Neurobiology and Jerry Lewis Neuromuscular Research Center, University of California, Los Angeles, CA 90024. Dr. Stimers' present address is Dept. of Physiology, Duke University Medical Center, Durham, NC 27710. Dr. Taylor's permanent address is Laboratory of Biophysics, National Institute of Neurological and Communicative Disorders and Stroke, National Institutes of Health, Bethesda, MD 20892.

scopic ionic currents or single channel records. This is especially true for states that are increasingly removed from the open state.

The rising phase is one feature of I_g that has implications for transitions between the most closed states. Armstrong and Gilly (1979) ruled out the possibility that the rising phase is due to an artifact of the subtraction procedure, as could have been the case in earlier work (Armstrong and Bezanilla, 1974) or from the clamp time constant (Bezanilla and Taylor, 1978). They concluded that the rising phase can be interpreted as the result of the early transitions being slower than transitions closer to the open state or being less voltage dependent (less charge per transition). Alternatively, Hoyt (1982) has suggested that the rising phase may be due to an artifact intrinsic to the membrane that results in the membrane potential near the voltage-sensitive gates being prevented from reaching its clamped value rapidly.

This article will evaluate these possibilities and present evidence that we believe proves that the rising phase is an artifact caused by the geometry of the squid axon and its surrounding connective tissue. A preliminary report of these results has appeared (Stimers et al., 1984, 1986).

METHODS

Currents were recorded from cleaned, internally perfused, voltage-clamped axons from the squid *Loligo pealei* using the methods of Bezanilla and Armstrong (1977) and Bezanilla et al. (1982) with the exceptions described below.

Pulse Generation and Recording Electronics

A hardware system for pulse generation, acquisition, and display was designed for use with a 16-bit microcomputer (Intel 8086-based Lightning-1, Lomas Data Products, Westboro, MA). The system used did not require dedicated control by the computer for pulse generation, acquisition, or display. The computer loaded a random access memory (RAM) with up to 2,048 pairs of amplitudes and durations. The possible durations for each pulse in a given sequence ranged from 0.2 μ s to 6.55 ms at the fastest and 6.55 ms to 7.16 s at the slowest. Under software control, the system was triggered to replay the stored information through a 12- or 16-bit digital-to-analog converter and programmable counter independently of the computer. The acquisition was triggered by the hardware to begin loading another RAM with data from a sample-and-hold and 12-bit analog-to-digital converter connected to the signal to be recorded. The rate of acquisition could range from 0.2 μ s to 6.55 ms/point for up to 8,196 points. The rate of acquisition was independent of the rate of pulse generation, provided that the pulses were sufficiently long to permit the acquisition of the data. After this RAM was filled, it was then read by the computer for processing, display on an oscilloscope, or storage on a floppy disk. For each pulse procedure, 1,200 points were acquired and stored with all the adjustable parameters for that pulse. Unless otherwise noted, the P-P/ ± 4 procedure was used (Bezanilla and Armstrong, 1977; Bezanilla et al., 1982). A master program written in a combination of the Microsoft FORTRAN and Assembly languages was used to drive the hardware for acquisition, pulse generation, display, and data storage.

K^+ , Na gating, and capacity currents were digitally sampled at 20, 2, and 1.2 μ s/point, respectively. To prevent aliasing, the currents were filtered below the Nyquist frequency before being sampled.

Solutions

All solutions used are listed in Table I and are referred to in the text and figure legends as "external solution//internal solution." Membrane potentials were not corrected for junction potentials.

Gating Current

In most experiments, I_g was recorded with 160 mM Cs inside and either Tris-seawater (SW) or one of the hyperosmotic solutions listed in Table I outside. For a few experiments, as noted in the text, the 160 Cs solution was diluted 10% with water. The charge for each I_g or capacity current (I_c) was determined by numerically integrating the currents for a period of time, usually 2–3 ms for I_g and 500–600 μ s for I_c .

K⁺ Washout and Accumulation in the F-H Space

K⁺ current (I_K) was recorded with 10 K Tris-SW//400 KFG or hyperosmotic 10 K Tris-SW//400 KFG. The pulse patterns used in determining washout and accumulation are

TABLE I
Solutions

Internal solutions*	K	Cs	TMA	TEA	F	Glutamate	Trizma-7.2 [‡]
400 KFG	400	0	0	0	100	300	10
160 Cs		160	70	20	100	150	10
External solutions			Ca	K	Tris [‡]	Cl	Tetrodotoxin
Tris-SW			50	—	475	575	0.0003
10 K Tris-SW			50	10	465	575	0.0003
Hyperosmotic Tris-SW			50	—	575	675	0.0003
Hyperosmotic 10 K Tris-SW			50	10	565	675	0.0003

All solutions were adjusted to an osmolality of 970 mosmol/kg except the hyperosmotic solutions, which had 10–20% higher osmolality. Internal pH, 7.3; external pH, 7.5. Concentrations are in millimolar. TMA, tetramethylammonium. TEA, tetraethylammonium.

* Osmolality adjusted with sucrose.

[‡] Tris(hydroxymethyl)aminomethane at pH 7.2 from Sigma Chemical Co. (St. Louis, MO).

[‡] Trizma base (Sigma Chemical Co.).

described in the Results. Reversal potentials for K⁺ were determined by measuring the amplitude of tail currents at two potentials (–80 and –30 mV) and assuming a constant conductance for the channels in this potential range.

RESULTS

We have observed in many axons that the gating current (I_g) sometimes does not have a rising phase. That is, in less than the 5–10 μ s necessary for V_m to reach the command potential, I_g is maximal. We have often observed the development of a rising phase on I_g in axons that initially have no rising phase. An example of this is shown in Fig. 1A with two superimposed I_g records from a single axon. We have also observed, in parallel with this change in I_g , that the capacity current (I_c) for a 10-mV hyperpolarizing pulse also has altered kinetics. Fig. 1B shows two superimposed records of I_c recorded from a single axon for a pulse from

–80 to –90 mV. The record of I_c labeled “early” corresponds to I_g without a rising phase. I_c appears as a single component that settles to the baseline in 5–10 μ s. The other record of I_c corresponds to the gating current with a rising phase; it has a prominent slow component that lasts 50–80 μ s. Also notice that the peak of the fast component decreases when the slow component increases.

These observations, we believe, suggest that the rising phase observed on I_g is not an intrinsic property of the channel but is rather an artifact. Previous work has shown that the rising phase is not due to the clamp time constant or the method used to subtract the voltage-independent components of I_c (Bezanilla and Taylor, 1978; Armstrong and Gilly, 1979). The fact that we can record I_g without a rising phase in fresh axons also argues that the clamp or the subtraction procedure cannot be responsible for the rising phase seen in the same axon late in the experiment. One possibility for the development of a rising phase with

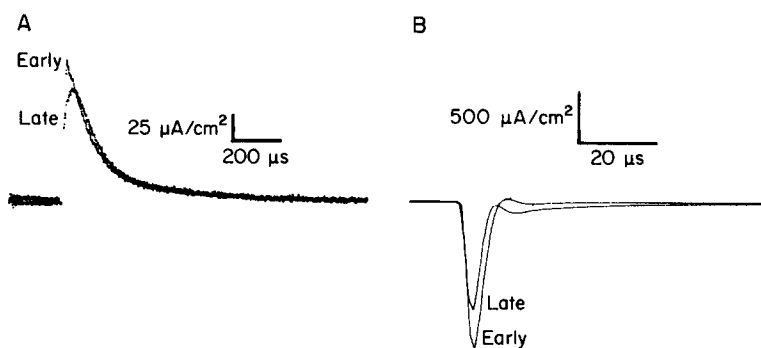


FIGURE 1. Gating current and capacity transient in a single axon that developed a rising phase with time. This figure shows gating currents (left) and capacity currents (right) both early and late in the experiment. Note the difference in time scale. It is shown that when the gating current has a rising phase, the capacity transient has a slow component. Gating currents are blanked for 12 μ s after the step. Solutions: Tris-SW//160 Cs. Subtracting holding potential, –150 mV. Holding potential, –70 mV, pulse to +50 mV for gating and –80 mV for capacity current.

time is that the platinum electrodes may become polarized and thus may be less efficient at passing current. We will present evidence that rules out this possibility. The fact that I_c has two components when I_g has a rising phase suggests that a region of the membrane is somehow isolated from the rest of the membrane and is being clamped more slowly. When the series resistance compensation was adjusted so that $\geq 90\%$ of the measured series resistance was compensated, the fast component of I_c was over in 5 μ s. However, the slow component was not significantly altered in either its amplitude or time course. Increasing the compensation above 100% caused the current to oscillate in the region between the fast and slow components. This can be observed to a small degree in Fig. 1B for the record labeled “late.” Here the compensation was adjusted so that a small notch is seen in the record. This notch is the beginning of instability in the clamp. The inability to alter the slow component of I_c further suggests that it is

due to a region of membrane that is isolated from the voltage-sensing electrodes under these conditions. Integration of I_c reveals that as much as 50% of the membrane was not well clamped for the first 100 μ s after a voltage step. We will show that this artifact can be removed.

Effect of Hyperosmotic External Solution

Fig. 2 illustrates what happens to I_c (A) and I_g (B) when the osmolality of the external solution is raised from ~ 970 to 1,100–1,200 mosmol (a 10–20% increase in osmolality) by the addition of 100 mM Trizma-7.2 to the solution. Fig. 2A shows two superimposed records of I_c from one axon. The lower trace was recorded in normal Tris-SW; notice the prominent slow component and the

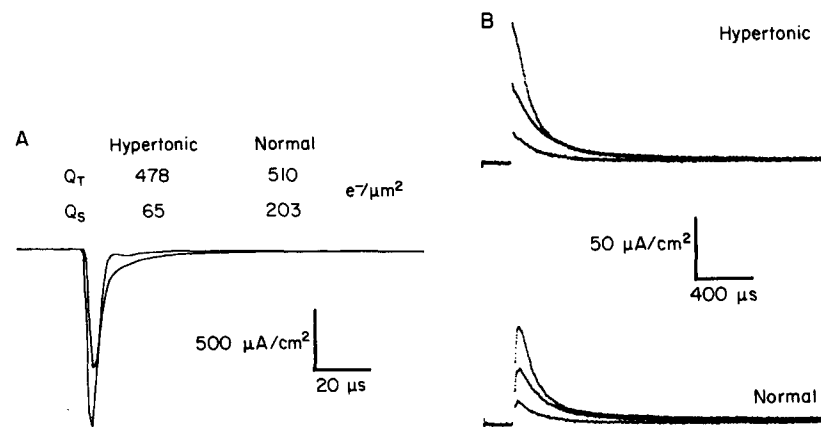


FIGURE 2. Capacity and gating currents change time course when hyperosmotic solution is applied. (A) In normal solution, I_c has a prominent slow component that is reduced by hyperosmotic solution without changing the total charge moved by the pulse from -70 to -80 mV. (B) I_g in the same axon shows that the rising phase is eliminated, making the external solution hyperosmotic with respect to the internal. Gating currents are blanked for 12 μ s after the step. Records illustrated for potentials of -30 , 10, and 50 mV from a holding potential of -70 mV. Solutions: Tris-SW//160 Cs or hyperosmotic Tris-SW//160 Cs. Subtracting holding potential, -150 mV.

decreased amplitude of the fast component. Switching the external solution to hyperosmotic Tris-SW resulted, after a delay of 10–15 min, in a rather abrupt change in the shape of I_c so that it appears primarily as a single fast spike. When both of these records are integrated, it can be seen that the total charge (Q_t) was not changed, but rather the distribution of the charge between the fast and slow components was changed. The amount of charge in the slow component (Q_s) decreased from 40% in normal Tris-SW to only 14% in hyperosmotic Tris-SW. Since Q_t was not changed by this treatment, neither the membrane area nor the capacitance appears to have been affected. If the axon was returned to normal Tris-SW again, then I_c reverted to its previous shape with two components. This change in I_c is completely reversible and does not depend on whether the axon was initially in hyperosmotic or normal solution. In one experiment, the solution

was changed five times and each time I_c changed as illustrated here. This reversibility argues against there being a problem with the platinum electrodes.

Fig. 2B shows, for the same axon as illustrated in Fig. 2A, that in normal solution, I_g had a prominent rising phase. Upon switching to hyperosmotic Tris-SW, the rising phase was virtually eliminated. Again, this change in the rising phase was completely reversible when the axon was returned to normal Tris-SW. These experiments have also been done when the external solution was made hyperosmotic by adding 200 mM sucrose or 100 mM NaCl or by making the internal solution hypoosmotic by dilution (10%) with water. The results were identical to those presented here. In all of these treatments, the only common factor is the presence of a water gradient that results in water flowing out of the axon. If the rising phase were due to the clamp or the subtraction procedure used, or even if there were a problem with the electrodes, then we would not expect those artifacts to be altered by making the external solution hyperosmotic with respect to the internal solution. If we had used only Trizma-7.2 to increase the osmolality, then it would be possible that the properties of the clamp could be altered by the increase in ionic strength of the solution; however, the use of sucrose to increase the osmolality and the dilution of the internal solution with water eliminates this possibility.

Since it appears that the time course of I_g is significantly different only at early times, we would like to know whether the fast component of I_g in hyperosmotic Tris-SW is an additional charge or simply results from a redistribution of the charge in time. Integration of the current records reveals that the total charge is not changed (Fig. 3). In addition, Fig. 3 illustrates that the voltage dependence of the charge movement is also not changed by this treatment. Note that the data are plotted as charges per square micron, not normalized to the maximum value. This is important to show that the amount of charge is not altered by hyperosmotic Tris-SW. Again, this argues against the rising phase being due to an artifact of the subtraction procedure. If subtraction were a problem, we would expect to see an increase in the total charge for the case when no rising phase is present, since the later time course of I_g should be affected to a much lesser degree by the subtraction procedure.

Inactivation of the Na Channel Affects the Rising Phase

Another experimental manipulation that is known to affect the rising phase of I_g is giving an inactivating prepulse before recording I_g (Armstrong and Bezanilla, 1977). In axons with an I_g that shows a rising phase, immobilization of the gating charge decreases the rising phase, as shown in the upper right of Fig. 4. In the same figure (left), it is shown that an identical pulse pattern given after the application of hyperosmotic solution outside results in I_g being faster after a prepulse. In both cases, as expected, the total charge moved after a prepulse is reduced because of the inactivation developed during the prepulse. Thus, the effects of a prepulse are qualitatively the same in both cases; with a prepulse, I_g becomes faster. As suggested by Armstrong and Gilly (1979), this is expected if the effect of inactivation is to restrict the channel to a small number of states. In the Discussion, we will show that the elimination of the rising phase and the

speeding up of the falling phase for the I_g without a rising phase can be explained by just this single mechanism of restricting the channel to a small number of states.

Washout of K^+ from the F-H Space

When the axon is bathed in 10–20% hyperosmotic solution, there will be water flowing out of the axon in the steady state. Because of this, we consider the possibility that the space between the axon and the surrounding Schwann cells (the F-H space, first postulated by Frankenhaeuser and Hodgkin, 1956) might be enlarged. This has previously been demonstrated by Adelman et al. (1977). To confirm this, we chose to use K^+ as a probe of the F-H space, first looking at the rate at which K^+ washes out of the space once loaded by a depolarizing

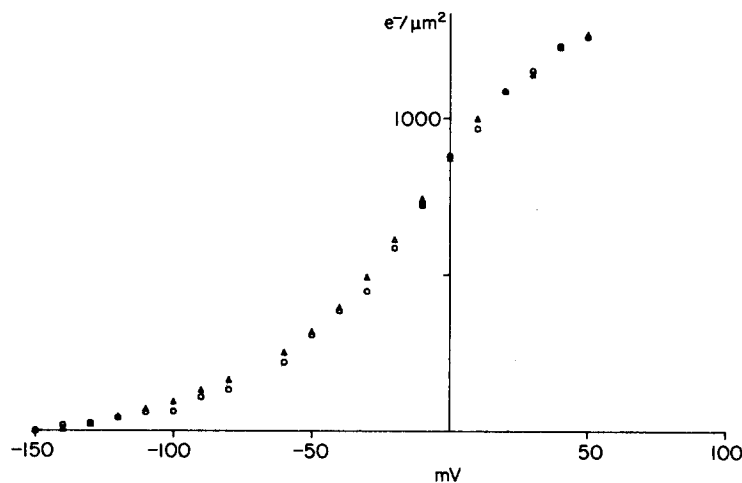


FIGURE 3. Charge vs. voltage curve is not affected by hyperosmotic solution in either its voltage dependence or quantity of charge moved. The two sets of data are not normalized; the curves are offset so that the charge at -150 mV was 0. In this axon, the external solution (Tris-SW) was made hyperosmotic by adding 200 mM sucrose. The effect is exactly the same if Tris is added instead.

prepulse and then looking at the rate at which the K^+ concentration increases in the F-H space. Using the Nernst equation with $[K^+]_i = 400$ mM and $[K^+]_o = 10$ mM, one calculates an expected reversal potential of -92 mV. Deviations from this are expected when long (50 ms) depolarizing pulses are given, which loads the F-H space with K^+ (Frankenhaeuser and Hodgkin, 1956; Adelman et al., 1973). As K^+ washes out of the space, E_K will return to the expected value. Assuming that the F-H space is well stirred and that the Schwann cells can be replaced by a thin membrane with no unstirred layer (see Taylor et al., 1980), the concentration of K^+ in the F-H space $[C(t)]$ can be expressed as:

$$C(t) = C_L e^{-t/\tau} + C_o, \quad (1)$$

where C_L and C_o are the concentrations of K^+ added to the space by the prepulse

and present in the external solution, respectively. From this and the Nernst equation, one can easily derive the following equation, which predicts the rate of recovery of the reversal potential as a function of time, $E_K(t)$:

$$\ln\left\{e^{[E_K(t)-E_K(\infty)]F/RT} - 1\right\} = \ln(C_L/C_o) - t/\tau, \quad (2)$$

where $E_K(\infty)$ is the reversal potential at infinite time and F , R , and T have their usual meanings. Plotting the left-hand side of this equation as a function of time,

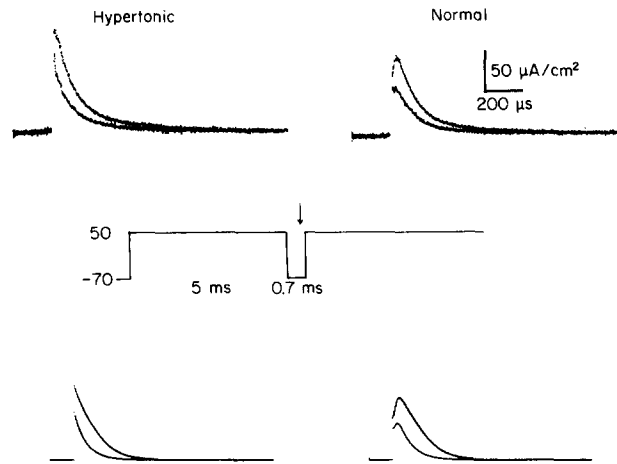


FIGURE 4. Effect of inactivation on rising phase. The upper part of the figure shows gating currents from a single axon taken with the pulse pattern shown in the middle of the figure. The data were recorded at the time indicated by the arrow either without the first pulse (larger currents) or with the prepulse (smaller currents: charge is immobilized by inactivation). Gating currents are blanked for 12 μ s after the step. The lower portion of the figure shows a simulation using the structural model presented later in this article (see Discussion) and the kinetic model presented by Stimers et al. (1985a). For the structural model, we used a value of $R_{FH} = 10 \Omega \cdot \text{cm}^2$ to simulate the case of having normal osmolarity present and $1 \Omega \cdot \text{cm}^2$ when there is hyperosmotic solution outside the axon. The parameters used for the kinetic model were:

Transition	d	z	W_α	W_β
1	0.3	1.0	20.80	21.00
2	0.3	1.0	20.00	21.30
3	0.3	1.0	20.00	21.60
4	0.3	1.0	19.90	21.90
5	0.3	1.0	19.75	22.20
6	0.3	1.0	19.60	22.50
(Inactivation)	1.0	1.0	22.23	20.44

where d is the distance through the field of the barrier, z is the valence of the charge moving in a given transition, W_α is the difference in units of kT from the well to the barrier peak of the forward reaction, and W_β is the equivalent term for the backward reaction. Solutions: Tris-SW//160 Cs (right) or hyperosmotic Tris-SW//160 Cs (left). The time scale applies to all records, but the current scale applies only to the data, not to the simulation, which is arbitrarily scaled.

we can determine the time constant for this process from the slope of the line. To evaluate Eq. 2, we measured $E_K(t)$ using the following procedure. The inset in Fig. 5A illustrates the pulse procedure used to measure the rate of washout.

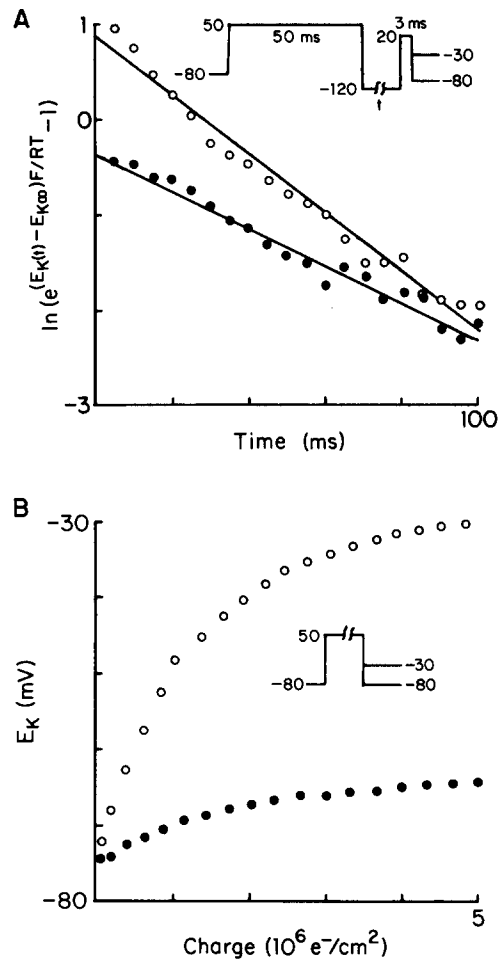


FIGURE 5. Accumulation and washout of K^+ . In both *A* and *B*, the open circles represent data from an axon in which the internal and external osmolalities were balanced. The filled circles represent data from an axon in which the external solution was hyperosmotic with respect to the internal solution. (*A*) Accumulation of K^+ in the F-H space. The inset at the top of the figure shows the experimental procedure used to obtain these data. The washout of K^+ was assumed to be a single-exponential process, as discussed in the text. The slope of each line is $-1/\tau$, the time constant. In normal solutions (Tris-SW//160 Cs) with a balanced osmolarity, the τ for accumulation was 32.5 ms. When the same axon was bathed in hyperosmotic Tris-SW, the rate of accumulation was slower ($\tau = 50.3$ ms). (*B*) Washout of K^+ from the F-H space. The inset shows the experimental procedure used to obtain these data. The graph clearly shows that this axon had a much greater amount of accumulation of K^+ in the F-H space when in normal solution (open circles) than in hyperosmotic solution (filled circles).

A 50-ms depolarizing prepulse is given to load the F-H space with K^+ . Then the membrane is stepped to -120 mV for a variable time (-120 mV is used so that the channels will close rapidly to minimize unloading). A brief test pulse is then given to activate the channels and the amplitude of the tail current is measured at two potentials, -80 and -30 mV. From these tail currents, one can easily calculate the reversal potential for K^+ . $E_K(\infty)$ was chosen to be the value of E_K 200 ms after the depolarizing prepulse (see Discussion). The graph shows the plot of Eq. 2 for hyperosmotic and normal external solutions. The line drawn is the linear regression of the data and τ is equal to minus the reciprocal of the slope of the line. The washout is $\sim 35\%$ faster for normal solution in this axon.

To explain these data, we must first consider that two effects of hyperosmotic solution may be operating during this experiment. First, if the F-H space expands, then the rate of washout will be slower since a larger volume is being washed. Second, if the Schwann cells shrink in the steady state, then the clefts may be larger, which will result in an increase in the rate of washout. Adelman et al. (1977) showed that both of these effects occur when axons are bathed 15 min in 1,250 mosmol artificial SW. Since these two physical changes have effects that

TABLE II
Washout of K^+ from the F-H Space

Axon	Normal		Hypertonic		θ_H/θ_N
	τ	$\ln(C_L/C_o)$	τ	$\ln(C_L/C_o)$	
	<i>ms</i>		<i>ms</i>		
WMAY245A	22.9	0.87	29.7	0.45	1.5
WMAY245B	29.3	0.85	31.6	-0.03	2.4
WMAY255A	38.9	1.09	55.8	0.12	2.6
WMAY255B	32.5	0.85	50.3	-0.33	3.2
Mean \pm SEM					2.5 ± 0.4

are in the opposite direction, it seems clear that the F-H space must be expanding under these conditions. Quantitatively, from the intercepts of the fitted lines with the ordinate, we calculate the ratio of the loading concentrations in the two conditions. Assuming that the surface area of the axon did not change in this experiment, then this ratio is equal to the ratio of the thickness of the F-H space (θ) in the two cases; in other words, this value indicates how much the F-H space expands in hyperosmotic 10 K Tris-SW. The ratio θ_H/θ_N for this axon was 3.5. Since there is the possibility that the clefts are enlarged in this experiment, this ratio is a minimum estimate for the increase in θ for this axon. The results for this and other axons are summarized in Table II, and provide an estimate of $\theta_H/\theta_N = 2.5 \pm 0.4$.

Accumulation of K^+ in the F-H Space

Further evidence that θ increases in hyperosmotic solution is provided by the rate of accumulation of K^+ in the F-H space. Fig. 5B illustrates these experiments. The accumulation of K^+ in the F-H space depends upon (a) the rate of loading and (b) the rate of washout of K^+ from the F-H space. The rate of K^+ loading is estimated from the change in E_K produced by the following procedure. The

inset of Fig. 5B shows that a depolarizing pulse was given for a variable duration (1–20 ms), after which the tail currents were measured at two potentials. For both hyperosmotic and normal solutions, we plot E_K as a function of the integral of I_K (charge per square centimeter) during the depolarizing pulse. This procedure is similar to that used by Adelman et al. (1973). Fig. 5B clearly shows that E_K , and therefore the concentration of K^+ in the F-H space, changes much more rapidly in normal solution than in hyperosmotic solution. The possible conclusions from these data are that the volume of the F-H space is increased or that the rate of washout is increased by hyperosmotic solution. Since we just showed in the previous section that the rate of washout is decreased by hyperosmotic solution, we conclude that the volume is increased under these conditions, which agrees with the findings of Adelman et al. (1973, 1977).

In this experiment, we can get a better estimate for θ since for short pulses the amount of K^+ that leaves the F-H space during the pulse is much smaller than the amount of K^+ that is loaded into the space by the pulse. From this observation,

TABLE III
Accumulation of K^+ in the F-H Space

Axon	Normal	Hypertonic	θ_H/θ_N
	<i>nm</i>	<i>nm</i>	
WMAY085B	15.5	66.4	4.3
WMAY115A	49.3	94.5	1.9
WMAY165A	26.4	143.0	5.4
WMAY255B	51.1	433.0	8.5
Mean \pm SEM	35.6 \pm 8.7	184 \pm 84	5.0 \pm 1.4

we can make a model-independent estimate of θ in each case using the following equation:

$$\theta = \frac{Q(t_2) - Q(t_1)}{C_{FH}(t_1) \left\{ e^{[E_K(t_2) - E_K(t_1)]F/RT} - 1 \right\}}$$

where Q is the number of particles (moles per square centimeter) injected into the F-H space by I_K at times t_1 and t_2 , $C_{FH}(t_1)$ is the concentration (moles per cubic centimeter) of K^+ in the F-H space at time t_1 , and E_K is the K^+ reversal potential. This equation assumes only that the surface area of the axon is not changed and that the times used are short compared with the rate of washout. For pulse durations <5 ms, we find that for the data in Fig. 5B, θ in normal solution was 26 nm, while θ in hyperosmotic solution was 143 nm, an increase of more than fivefold. The results from this axon and others are summarized in Table III. We find that θ increased by 5.0 ± 1.4 -fold. This value is in good agreement with the data of Adelman et al. (1977). Their relation for θ and osmolality would predict an increase in θ of 3.9-fold using the osmolalities of our solutions; this value is between the two values (2.5 and 5.0) that we report.

DISCUSSION

Since I_g was first measured, there has been a considerable discussion about whether or not there is a rising phase. We have shown here that the rising phase

can be eliminated by making the external solution 10–20% hyperosmotic with respect to the internal solution. The time course for elimination of the rising phase on I_g was quite variable. It appeared as a sudden change after a variable delay, rather than as a gradual change over a long period of time. This suggests the possible involvement of some sort of cell glue, which we will not speculate on because of a lack of data.

Armstrong and Gilly (1979) showed that the rising phase could be accounted for simply by making the first transition from the most closed state to the next state slow compared with subsequent transitions. Simulations using the model presented by Stimers et al. (1985a) also result in a rising phase when the first activating step is made slower than subsequent transitions. If this were the mechanism of the rising phase, then we would have to postulate that the rate constants of the first transition in the opening process were altered by water flow across the axon membrane. We have no evidence either to support or to refute this hypothesis; however, we feel that a simpler explanation of the data is more likely. Furthermore, Armstrong and Gilly (1979) found no evidence that the rising phase was due to an artifact of the subtraction procedure or of the clamp electronics. We also confirm this since the treatment with hyperosmotic external solution was able to reversibly eliminate the rising phase.

Hoyt (1982) has suggested that the rising phase of I_g might be due to a dielectric relaxation process within the membrane not associated with I_g but due rather to some other membrane component. This relaxation would cause the membrane potential in the region of the gating apparatus to change more slowly than the command pulse. This alteration of the membrane potential would then result in a rising phase on I_g . We agree with her description of the phenomenon, but believe that the mechanism is due to an extrinsic relaxation process that is associated with the resistance of the F-H space. It has been shown here that in response to the application of hyperosmotic solution outside the axon, water flowing out of the axon increases the volume of the F-H space, primarily its thickness, and therefore decreases its resistance. Before discussing this model in further detail, we would like to discuss the evidence that justifies our conclusion that the F-H space expands.

Osmotic Pressure in the F-H Space

In the Appendix, we present a full derivation for the osmotic pressure in the F-H space; here we present a summary of that derivation. Assuming that the Schwann cells are of uniform size and spacing, one can solve for the movement of both water and solutes across the axon membrane, through the clefts between the Schwann cells and through the Schwann cell membrane. Since, in the steady state, movement of water and solutes into the F-H space must be equal to movement out of the space, one can solve for the change in pressure (P) in the F-H space caused by a given osmotic gradient across the axon membrane and the velocity of water in the clefts (v) (see Eqs. A2 and A3 in the Appendix). Solving these equations for P and v , one can then calculate the concentration in the F-H space (C_{FH}) (see Eq. A1 in the Appendix). Solving these equations for our case of having the external solution hyperosmotic by 10–20% with respect

to the internal solution, we find that P is always positive and C_{FH} is nearly equal to C_o . This result suggests to us that the volume of the F-H space must be increased by treatment with hyperosmotic solution. We are not able to say from this model how much the space might expand, since the volume is always multiplied by an unknown elasticity factor for the Schwann cells and connective tissue. If the volume of this space is changing significantly, then it could contribute to a series resistance for the regions of the axon membrane that are distant from the clefts. Adelman et al. (1977) presented anatomical evidence showing that θ may be linearly related to the osmolality of the external solution over a range that is close to that used by us. Their relation predicts that θ would increase 3.9-fold under our conditions, which agrees very well with our values of 2.5 and 5.0.

K⁺ Washout and Accumulation

Since the simulation of water flow suggests that there is an increase in the pressure in the F-H space when hyperosmotic solution is applied externally, it seems reasonable to assume that the thickness of the F-H space is increased under these conditions. To demonstrate this experimentally, the rate of washout and the amount of accumulation of K^+ were measured and, as shown in the Results, both values were decreased. A reasonable assumption for the effect of hyperosmotic solution on the Schwann cells is that in the steady state they should either shrink or remain the same volume as in normal solution (Adelman et al., 1977). If this were the case, then since the time constant for washout is proportional to the ratio of the thickness of the F-H space (θ_H/θ_N) and the width of the clefts (Frankenhaeuser and Hodgkin, 1956; Taylor et al., 1980), we would expect that θ must be increased. From this model, we obtain a minimum estimate of the increase in θ to be a factor of 2.5 ± 0.4 .

In doing these experiments, we did not intend to completely describe the process by which K^+ diffuses from the F-H space. The assumption we made was that the model used by Frankenhaeuser and Hodgkin (1956) would give a reasonable approximation to this process (Taylor et al., 1980). However, we noticed some discrepancies, which we shall discuss. First, the assumption that there is a single-exponential process governing the washout seems to be inaccurate. We were able to measure the effects of a 50-ms depolarizing prepulse on the reversal potential for intervals between the prepulse and test pulse as long as 1 s at -120 mV. If there were only a 1-mV change in the reversal potential 1 s after the prepulse, then from Eq. 2 we would calculate a time constant of ~ 300 ms (the exact value depends upon the value chosen for the ordinate intercept). This leads to the next problem: choosing the value for $E_K(\infty)$. If the measured value for $E_K(\infty)$ (E_K measured by the test pulse without a prepulse) is used, then the data plotted in Fig. 5A would appear upwardly concave, which would indicate a multiexponential process for the washout of K^+ from the F-H space. We therefore chose to use the value of E_K at 200 ms. This is arbitrarily chosen but it does have the benefit of making the results easy to interpret. The result of this is to underestimate the time constant for a single exponential. Since these slower components appeared to be present for both conditions and we are not attempt-

ing to characterize the diffusion barriers of the F-H space, we do not feel that the errors significantly affect the conclusions, but the estimate for the change in θ is probably an underestimate.

In the accumulation experiments, qualitatively, the result is obvious that θ is increased by hyperosmotic solution. In this experiment, however, a better estimate for θ is obtained since fewer assumptions are made. Assuming no change in surface area caused by the treatment with hyperosmotic solution (which is supported by the fact that the charge carried by I_c remains constant) and assuming that the measurements are made at times short relative to the time constant for washout, we calculate that θ increases 5.0 ± 1.4 -fold in hyperosmotic solution.

Model for F-H Space Resistance

Fig. 6 illustrates a simplified model of a physical system that will account for the data. The figure shows a cleft between two Schwann cells that would contribute

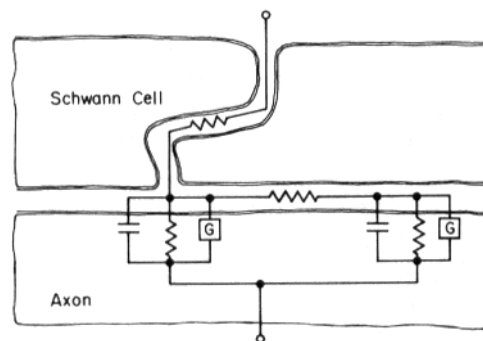


FIGURE 6. Simplified structural model of the axon and surrounding Schwann cells. This model depicts a simplified structural arrangement that can explain the data presented in this article. Two patches of axon membrane are shown that are isolated from each other by a resistance owing to the F-H space. The magnitude of this resistance is dependent upon the osmotic gradient across the axon membrane. See text for further discussion.

to the normal series resistance (R_s) of $\sim 4 \Omega \cdot \text{cm}^2$. The cleft is continuous with the F-H space, which is between the Schwann cells above and the axon membrane below. The resistance of the F-H space (R_{FH}) is variable, depending upon its volume and the resistance of the solution in it. Since R_s can be compensated for electronically, the patch of membrane close to the cleft will be clamped with a square potential that rises with the speed of the clamp—in our case, $\sim 5 \mu\text{s}$ (the duration of the fast component of I_c). R_{FH} , on the other hand, cannot be compensated, since this would result in an overcompensation of R_s . Therefore, the second patch of membrane, which is removed from the cleft by R_{FH} , will be clamped with a command voltage that will relax with a time constant determined by the product of R_{FH} and the membrane capacitance. Obviously, in the real situation, R_{FH} must be a continuous gradient of resistance separating an infinite number of small patches of membrane, so the specific details of the simulation should not be considered, only the qualitative way in which it can account for

the data. We will show that the two-patch model is an adequate approximation for the present discussion.

We have simulated the predictions of this model for the case in which R_{FH} is both large ($10 \Omega \cdot \text{cm}^2$) and small ($1 \Omega \cdot \text{cm}^2$). This was done using the sequential model presented by Stimers et al. (1985a) and solving it by two methods that represent the solution of each patch of membrane: (a) a numerical solution is obtained for a command voltage that rises with a time constant determined by the product of the membrane capacitance and R_{FH} ; (b) an exact solution is obtained for an instantaneous voltage jump. The sum of these two methods gives the solution for the entire model. The results of this simulation are shown in the lower part of Fig. 4 for two pulse patterns as indicated in the figure. The left-hand traces represent the case when R_{FH} is small; notice the lack of a rising phase in either case. On the right we illustrate the simulation for the case when R_{FH} is large. The larger trace in each part of this figure is for the case when a single pulse from -80 to $+50$ mV is given to elicit the gating current. The smaller traces represent the case when I_g has been inactivated by a prepulse (see inset and figure legend). Comparing these simulations with the data in the upper part of Fig. 4, one can easily see that this model qualitatively accounts for the experimental observations, although the precise kinetic detail is not exactly matched. One point not illustrated here, which is also predicted by this model, is that the rising phase is smaller for less strongly depolarizing pulses. Since one must consider that the total capacity current must flow through R_{FH} , not just I_g , it seems reasonable that for larger pulses the voltage drop across R_{FH} will be larger; this will result in greater distortion of the time course of I_g at early times.

As suggested by Armstrong and Gilly (1979), the lack of a rising phase when I_g is immobilized can be explained by the channel being restricted to only a few states. This emphasizes an important observation about the difference in the rising phase in I_g in the two cases, inactivated and noninactivated. In the case of the Armstrong-Gilly model, the rising phase for noninactivated I_g is due primarily to the transition between states X_6 and X_5 , although, strictly, all the transitions are involved in determining the eigenvalue responsible for the absence of a rising phase. When inactivated, the absence of a rising phase results from the channel being restricted to only one transition (between states X_2Z and X_1Z). This is in contrast to the interpretation of Bekkers et al. (1984). They have misinterpreted the predictions of the simultaneous differential equations that describe the model of Armstrong and Gilly (1979), such that the weighting of the eigenvalues by the initial conditions was ignored in their treatment.

Furthermore, the reason that the inactivated I_g decays faster is that the inactivated system is essentially reduced to a single-exponential process, whereas the noninactivated system has multiple exponentials, for which each time constant is a function of all the rate constants. This is easily seen in our data and is predicted by our model (Fig. 4). Mathematically, the system is forced to be slower when there are multiple sequential processes than when only a single-exponential process is present, unless that process is extremely slow. Since the rate constants of an extremely slow process would dominate the time course of activation in the absence of inactivation, such a slow process cannot be present. These points are clearly in disagreement with the analysis of Keynes et al. (1982) and Greef

et al. (1982). These authors have undertaken the fractionation of the gating current into inactivating and noninactivating components by subtracting the noninactivating I_g from the total I_g . Since the kinetic components of these two measurements of I_g are so different, we have serious questions about the meaning of their analysis.

In summary, we report here evidence that compels us to conclude that the Na channel gating current in squid giant axon does not have a rising phase. The reported rising phase is due to an artifact of uncompensated series resistance caused by the F-H space. This resistance is easily reduced to low values by the application of a 10–20% water gradient across the axon membrane such that the external solution is hyperosmotic with respect to the internal solution. We find that all the data can be explained by a model in which the membrane is divided into two patches isolated by a resistance between them. The data are also consistent with a linear sequential model with parallel inactivation and we find no evidence to suggest that the gating current is composed of two separable components. The implications of these results are several. (a) If ionic currents are measured when I_c has a slow component, then the time course and voltage dependence should be altered, since R_{FH} must be slowing down the voltage applied to a region of membrane and preventing the membrane potential from reaching its command value owing to the large voltage drop across R_{FH} . For currents as large as 5 mA/cm², the membrane would be out of control by 50 mV if R_{FH} is 10 $\Omega \cdot \text{cm}^2$. (b) When implications are being drawn about the early time course of I_g , one must be careful that R_{FH} is small. For example, the data of Bezanilla and Taylor (1978) may need reinterpretation as to the effect of temperature on the early time course of the gating current. If R_{FH} was large (as suggested by the rising phase), then its slowing effect may be responsible for making the early time course of I_g apparently less temperature sensitive. (c) Frequency domain measurements of the lossy capacitance of the membrane may be in error, since R_{FH} would appear as a lossy capacitance. This property is being looked at by us now and the preliminary results suggest that this is indeed the case (Stimers et al., 1985b).

APPENDIX

F-H Space Water Movement Including Solvent Drag: Steady State

We want to consider the effects of changes in the osmolality of the external solution on the longitudinal resistance of the Frankenhaeuser-Hodgkin (F-H) space. Increasing the osmolality of the external solution with respect to that inside the axon will cause a steady outward movement of water. We ask what effect this water movement will have on the volume of the F-H space and on the concentration of ions within it.

The squid axon is surrounded by a layer of Schwann cells enclosed by a basement membrane and connective tissue. For the model that we will consider, we will ignore the basement membrane, connective tissue, and the unstirred layer. The Schwann cells are considered to be all of the same size and the clefts are considered to be straightened. The axon membrane is taken to be planar and gradients perpendicular to the plane of the figure are ignored. The length and width of the clefts and the distance between them will be average values. Some changes in the volume of the Schwann cells are to be expected, but we will not consider them here. One reason for this is that the experimental results

are similar whether the outward movement of water is the result of increasing the tonicity outside or reducing it inside.

We will include the effect of water movement through the Schwann cell itself. The glossary below defines the terms used in the following equations and gives the nominal values used in the calculations.

Glossary

h	width of cleft, 30 nm
L	length of cleft, 5.4 μm
b	distance between clefts, 13 μm
V	volume of F-H space per square centimeter of nerve membrane
V_e	equilibrium volume of the F-H space, when $P = 0$, 2.0×10^{-6}
P	excess pressure in the F-H space, dyn/cm ²
r	factor for elasticity such that $P = RT r (V - V_e)$, where R is the gas constant, T is absolute temperature, and RT is taken to be 2.353×10^{10}
D_o	diffusion coefficient of water, 2.44×10^{-5} cm ² /s
D_s	diffusion coefficient of solute, 1.0×10^{-5} cm ² /s
v	average velocity of water between two parallel surfaces, cm/s
v^*	D_o/L
v^{s*}	D_s/L
e	viscosity of water, 0.01 g/cm · s
C_i	concentration inside axon, mol/cm ³
C_o	concentration outside, mol/cm ³
C_{FH}	concentration in the F-H space, mol/cm ³
C_{H_2O}	concentration of pure water, 0.0556 mol/cm ³
P_n	permeability of nerve membrane to water, 0.001 cm/s
P_s	permeability of Schwann cell membrane to water, 0.001 cm/s
M	$= h^3 RT / 12 b e L$

Flow of Solute from the F-H Space to Outside (F_c)

If the F-H space expands because of water flow and a pressure builds up in this space, the water will flow outward through the clefts with a velocity v . The equation for diffusion of a solute with concentration C along a distance x with velocity v is (Bean, 1972):

$$D_s \frac{\partial^2 C}{\partial x^2} - v \frac{\partial C}{\partial x} = \frac{\partial C}{\partial t}$$

For $C(t=0) = C_{FH}$ and $C(L) = C_o$, the solution for the steady state, $\partial C / \partial t = 0$, is not difficult (see Bean, 1972, p. 15), and we can write, for the flow of solute in a cleft:

$$F_c = v(C_{FH} e^{v/v^{s*}} - C_o) / (e^{v/v^{s*}} - 1).$$

In the steady state, $F_c = 0$, so

$$C_{FH} e^{v/v^{s*}} - C_o = 0, \text{ or } C_{FH} = C_o e^{-v/v^{s*}}. \quad (\text{A1})$$

Flow of Water across the Nerve Membrane (F_{w1})

Water will flow across the nerve membrane because of a hydrostatic pressure gradient and a diffusive effect. The outward diffusive flow will be:

$$P_n [(C_{H_2O} - C_i) - (C_{H_2O} - C_{FH})] = P_n (C_{FH} - C_i).$$

For certain water flows, the F-H space will expand but there must be a restoring elasticity so that a pressure, P , will build up. For permeability P_n , the outward flow will be $-P_n P /$

RT. We thus have that the total outward flow is:

$$F_{w1} = P_n(C_{FH} - C_i) - P_n P/RT.$$

The outward flow of water, $P_n(C_{FH} - C_i)$, will turn out to be $\sim 1,000$ times the inward flow caused by pressure, in our case, so the question of the permeability coefficient, P_n , being the same for diffusion or pressure flow becomes somewhat academic.

Flow of Water from the F-H Space to Outside (F_{w2} , F_{w3})

If we assume, for the model, that a cleft is a space between two parallel plates a distance h apart and the cleft has a length L , then for a pressure difference P between the ends of the cleft, the average velocity of flow of water will be given by (see Landau and Lifshitz, 1959, p. 55):

$$v = (h^2/12\epsilon L)P,$$

where ϵ is the viscosity of water. The amount of water flowing out owing to the pressure difference will be this velocity times the concentration of water in the F-H space [i.e., $v(C_{H_2O} - C_{FH})$].

There is also diffusion of water owing to an osmotic gradient in the cleft. Since the concentration of water in the F-H space is $(C_{H_2O} - C_{FH})$ and the concentration outside is $(C_{H_2O} - C_o)$, the diffusive flow will be given, as above for the solute diffusion, by:

$$v[(C_{H_2O} - C_{FH})e^{v/v^*} - (C_{H_2O} - C_o)]/(e^{v/v^*} - 1).$$

Substituting $C_{FH} = C_o e^{-v/v^*}$ from above, we see that the diffusive flow is equal to:

$$vC_{H_2O} - vC_o(e^{-v/v^*}e^{v/v^*} - 1)/(e^{v/v^*} - 1).$$

Adding the water flow owing to a pressure gradient to the diffusive flow, we have the flow in a single cleft. The flow per square centimeter is this flow times an area factor (h/b). We thus have:

$$F_{w2} = (h/b)v \left[2C_{H_2O} - C_o e^{-v/v^*} - \frac{C_o (e^{-v/v^*}e^{v/v^*} - 1)}{e^{v/v^*} - 1} \right].$$

If we assume that the pressure and concentration within the Schwann cell is constant and the permeability of the membrane is P_s , then the flow of water through this cell will be:

$$F_{w3} = [P_s(C_{FH} - C_o) - P_s P/RT]/2.$$

Calculation of P/RT and C_{FH}

Recalling that $v = (h^2/12\epsilon L)P$, if we define $M = h^3 RT/12\epsilon L$, we get $(h/b)v = MP/RT$.

The water flowing into the F-H space must, in the steady state, equal the water flowing out, so $F_{w1} = F_{w2} + F_{w3}$. Taking F_{w1} , F_{w2} , and F_{w3} from above, we can solve for P/RT , with $C_{FH} = C_o e^{-v/v^*}$, and get:

$$P/RT = \frac{C_o e^{-v/v^*} - C_i - W}{1 + (M/P_n)(2C_{H_2O} - XC_o e^{-v/v^*})}, \quad (A2)$$

where

$$\begin{aligned} W &= P_s C_o / [2P_n(1 - e^{v/v^*})] / [1 + (P_s/2v^*)], \\ X &= 1 + (e^{v/v^*} - e^{-v/v^*}) / (e^{v/v^*} - 1), \\ v &= (h^2/12\epsilon L)P, \end{aligned} \quad (A3)$$

and we can solve for P and v . Knowing v , we can immediately calculate C_{FH} .

For the nominal values given above, if the internal solution concentration (C_i) is 980 mosmol and the external (C_o) is 1,100 mosmol, we get $P = 2.402$ (inches of H_2O) and $C_{FH} = 1,080$ mosmol. We also get $v = 3.53 \times 10^{-4}$ cm/s and $X = -0.4528$, so in the above expression $XC_o e^{-v/v^*} = -4.98 \times 10^{-4}$, which is very small compared with $2C_{H_2O} = 1.11$. This means that the difference between the diffusion coefficient of solute and water is inconsequential.

The solution for the transient case for diffusion with water flow in the cleft would be difficult. It is not intuitively clear whether or not the single membrane approximation for the clefts would be accurate at short times (see, e.g., Taylor et al., 1980).

This work was supported by National Institutes of Health fellowship to J.R.S. and by U.S. Public Health Service grant GM-30376.

Original version received 17 October 1985 and accepted version received 29 July 1986.

REFERENCES

- Adelman, W. J., J. Moses, and R. V. Rice. 1977. An anatomical basis for the resistance in series with the excitable membrane of the squid axon. *Journal of Neurocytology*. 6:621-646.
- Adelman, W. J., Y. Palti, and J. P. Senft. 1973. Potassium ion accumulation in a periaxonal space and its effects on the measurement of membrane potassium ion conductance. *Journal of Membrane Biology*. 13:387-410.
- Armstrong, C. M., and F. Bezanilla. 1973. Currents related to movement of the gating particles of the sodium channels. *Nature*. 242:459-461.
- Armstrong, C. M., and F. Bezanilla. 1974. Charge movement associated with the opening and closing of the activation gates of the Na channels. *Journal of General Physiology*. 63:533-552.
- Armstrong, C. M., and F. Bezanilla. 1977. Inactivation of the sodium channel. II. Gating current experiments. *Journal of General Physiology*. 70:567-590.
- Armstrong, C. M., and W. F. Gilly. 1979. Fast and slow steps in the activation of sodium channels. *Journal of General Physiology*. 74:691-711.
- Bean, C. P. 1972. The physics of porous membranes: neutral pores. In *Membranes: A Series of Advances*. G. Eisenman, editor. Marcel Dekker, Inc., New York. 1:1-54.
- Bekkers, J. M., N. G. Greeff, R. D. Keynes, and B. Neumcke. 1984. The effect of local anaesthetics on the components of the asymmetry current in the squid giant axon. *Journal of Physiology*. 352:653-668.
- Bezanilla, F., and C. M. Armstrong. 1977. Inactivation of the sodium channel. I. Sodium current experiments. *Journal of General Physiology*. 70:549-566.
- Bezanilla, F., and R. E. Taylor. 1978. Temperature effects on gating currents in the squid giant axon. *Biophysical Journal*. 23:479-484.
- Bezanilla, F., R. E. Taylor, and J. M. Fernandez. 1982. Distribution and kinetics of membrane dielectric polarization. I. Long-term inactivation of gating currents. *Journal of General Physiology*. 79:21-40.
- Frankenhaeuser, B., and A. L. Hodgkin. 1956. The after-effects of impulses in the giant nerve fibers of *Loligo*. *Journal of Physiology*. 131:341-376.
- Greeff, N. G., R. D. Keynes, and D. F. vanHelden. 1982. Fractionation of the asymmetry current in the squid giant axon into inactivating and non-inactivating components. *Proceedings of the Royal Society of London, Series B*. 215:375-389.
- Hoyt, R. C. 1982. Origin of the rising phase of gating currents. *Biophysical Journal*. 40:251-254.
- Keynes, R. D., N. G. Greeff, and D. F. vanHelden. 1982. The relationship between the

- inactivating fraction of the asymmetry current and gating of the sodium-channel in the squid giant-axon. *Proceedings of the Royal Society of London, Series B.* 215:391-404.
- Keynes, R. D., and E. Rojas. 1973. Characteristics of the sodium gating current in the squid giant axon. *Journal of Physiology.* 233:28P-30P.
- Keynes, R. D., and E. Rojas. 1974. Kinetic and steady-state properties of the charged system controlling sodium conductance in the squid giant axon. *Journal of Physiology.* 239:393-434.
- Landau, L. D., and E. M. Lifshitz. 1959. Fluid Mechanics. Pergammon Press, New York.
- Meves, H. 1974. The effect of holding potential on the asymmetrical displacement current in giant axons of *Loligo forbesi*. *Journal of Physiology.* 267:377-393.
- Stimers, J. R., F. Bezanilla, and R. E. Taylor. 1984. Squid axon sodium channel: gating current without rising phase. *Biophysical Journal.* 45:12a. (Abstr.)
- Stimers, J. R., F. Bezanilla, and R. E. Taylor. 1985a. Sodium channel activation in the squid giant axon. Steady state properties. *Journal of General Physiology.* 85:65-82.
- Stimers, J. R., F. Bezanilla, and R. E. Taylor. 1985b. Frequency domain measurements of membrane capacitance in squid axons with and without rising phase on the gating current. *Biophysical Journal.* 47:31a. (Abstr.)
- Stimers, J. R., F. Bezanilla, and R. E. Taylor. 1986. Sodium gating currents without rising phase: evidence from potassium currents. *Biophysical Journal.* 49:384a. (Abstr.)
- Taylor, R. E., F. Bezanilla, and E. Rojas. 1980. Diffusion models for the squid axon Schwann cell layer. *Biophysical Journal.* 29:95-118.